Electronic Supplementary Material (ESI) for Journal of Materials Chemistry A.

Supporting Information for

General flux-free synthesis of single crystal Ni-rich layered cathodes by employing Li-containing spinel transition phase for lithium-ion batteries

Feng Li[a,1], Ke Fan[b,1], Yuhang Tian[a,1], Peiyu Hou[a,*], Haiyan Zhang[c], Yanyun Sun,[d] Jinzhao Huang[a], Xijin Xu[a,*], Haitao Huang[b,*]

[a]School of Physics and Technology, University of Jinan, Jinan, 250022, China

E-mail: sps_houpy@ujn.edu.cn (P. Hou); sps_xuxj@ujn.edu.cn (X. Xu)

[b]Department of Applied Physics and Research Institute of Smart Energy, The Hong Kong Polytechnic University, Hong Kong, China

E-mail: aphhuang@polyu.edu.hk (H. Huang)

[c]School of Materials and Energy, Guangdong University of Technology, Guangzhou, 510006, China

[d]School of Automobile and Traffic Engineering, Jiangsu University of Technology, Jiangsu Province 213001, China

[1] These authors contribute equally to this work.

Experimental

Preparation of precursors and single crystal cathodes: Ni-poor and Ni-rich precursors $[Ni_{0.2}Co_{0.4}Mn_{0.4}](OH)_2$ and $[Ni_{0.6}Co_{0.2}Mn_{0.2}](OH)_2$ were preliminarily prepared *via* coprecipitation reactions. The preparative route of aimed precursors can be referred to our previous work.[1] Single crystal spinel oxide $Li[Ni_{0.4}Co_{0.8}Mn_{0.8}]O_4$ is firstly sythsized as a transition phase for the preparation of single crystal Ni-rich oxides. Namely, the precursors mixed with stoichiometric Li_2CO_3 (Li/TM=0.5) were calcined at 1000 °C for 4h. After that, the spinel oxide and stoichiometric $Ni(OH)_2$ ($Li_{0.5}TMO_2/Ni(OH)_2$=1:1) were added into deionized water, in which a small amount of polyvinyl pyrrolidone (PVP) as binder were also added. The mixture was further stirred and dried at 100 °C to form the spinel/$Ni(OH)_2$ composite. Finally, the composite mixed with stoichiometric Li_2CO_3 (Li/TM=0.5) was calcined at 850 °C for 20h under pure oxygen atmosphere to prepare single crystal Ni-rich oxide $Li[Ni_{0.6}Co_{0.2}Mn_{0.2}]O_2$. The polycrystalline Ni-rich oxide $Li[Ni_{0.6}Co_{0.2}Mn_{0.2}]O_2$ was also prepared from secondary particles of precursors at 850 °C for 20h under pure oxygen atmosphere. If we increased the molar ratio of spinel oxide and $Ni(OH)_2$ ($Li_{0.5}TMO_2/Ni(OH)_2$=1:3) and decreased the calcined temperature (800 °C), single crystal Ni-rich $Li[Ni_{0.8}Co_{0.1}Mn_{0.1}]O_2$ was also prepared. Due to lithium volatilization during solid-state reactions, 5% excess lithium source was added during all of calcination processes.

Materials characterization: The stacking density (ρ_s) of both cathodes was measured with tap-density tester (ZS-201, Liaoning Instrument Co. Ltd.). The morphology analysis and phase measurement of spinel and layered oxides were investigated by scanning electron microscopy (SEM, JMS-6700F and Hitachi S4800) and X-ray diffraction (XRD, Rigaku SmartLab). The fine structure and selected area electron diffraction (SAED) of single crystal was analyzed by high resolution transmission electron microscopy (HRTEM, JEOL JEM-2100F). The chemical compositions of Ni-rich oxides and elements dissolved into electrolyte after 100 cycles were measured by inductively coupled plasma optical emission spectrometry (ICP-OES, Agilent 5100). The valence states of elements on the grain surface were analyzed by X-ray photoelectron spectroscopy (XPS, Thermo Escalab250). The specific surface area of single crystal was measured by N_2 adsorption/desorption isotherm (Quantachrome NOVA). For differential scanning calorimetry (DSC) measurement, both NCM622 electrodes were initially charged to 4.4 V (Li/Li^+) at 0.1C in half cells, after which the delithiated cells were disassembled in an Ar-filled glovebox. Meanwhile, these materials were scraped off from Al foil and enclosed into a high-pressure crucible. Last, the DSC analysis was performed by a NETZSCH 204F1 instrument at a rate of 10 °C min^{-1} from 100 to 300 °C. The XRD analysis was performed by a Smart Lab diffractometer (Rigaku Japan), equipped with a Cu K_α radiation (λ= 1.54186 Å) and a HyPix-3000 detector. XRD data collection was performed by a step scan mode with a step size of 0.02° and a retention time of 1s between 10° and 80°. The Rietveld refinement of XRD was performed by Fullprof software package.

Computational details: The theoretical calculations were performed in the framework of density functional theory (DFT) implemented in the Vienna *ab initio* simulation package (VASP).[2,3] The generalized gradient approximation (GGA)+Uwith the Perdew-Burke-Ernzerhof (PBE) flavour was chosen as the exchange-correlation functional,[4-6] in which, the Hubbard U parameters for the *d*-orbitals of Ni, Co and Mn were set to 6.2, 3.32 and 3.9 eV, respectively.[7] For geometry optimization, the plane-wave cut-off energy of 450 eV was employed. A 5×1×1 supercell was built for the layer structure $Li[Ni_{0.6}Co_{0.2}Mn_{0.2}]O_2$ and $Li[Ni_{0.2}Co_{0.4}Mn_{0.4}]O_2$, and a 2×1×1 supercell was built for spinel structure $LiNi_{0.4}Co_{0.8}Mn_{0.8}O_4$. The Brillouin-zone was sampled using 3×13×3 Monkhorst-Pack grid for $Li[Ni_{0.6}Co_{0.2}Mn_{0.2}]O_2/Li[Ni_{0.2}Co_{0.4}Mn_{0.4}]O_2$ system and 2×3×3 for $Li[Ni_{0.4}Co_{0.8}Mn_{0.8}]O_4$ system. The convergence criterion for energy was set to be 10^{-5} eV and that for force was set as 0.01 eV $Å^{-1}$. Spin polarization was considered in the calculations.

To investigate the thermal stability, the ab initio molecular dynamics (AIMD) simulations with Nosé–Hoover thermostat for NVT ensemble were carried out at 1300 K with the time step of 2 fs and the total simulation time was set as 10 ps. Nosé mass corresponding to 80 fs (40 time steps) was chosen. VASP code was used for all the simulations.

The surface energy of facet (hkl) γ_{hkl} can be defined as follows:

$$\gamma_{hkl} = \frac{E_{hkl,slab} - E_{bulk}}{2A_{slab}}$$

where $E_{hkl,slab}$ and E_{bulk} represent the total energy of the slab model and bulk system, and A_{slab} is the surface area of the slab.

The formation energy ΔE was calculated by:

$$\Delta\mathrm{E} = E_{\mathrm{Li}[Ni_aCo_bMn_c]O_d} - (E_{Li} + aE_{Ni} + bE_{Co} + cE_{Mn} + dE_O)$$

here, $E_{\mathrm{Li}[Ni_aCo_bMn_c]O_d}$ are the total energies of $\mathrm{Li[Ni_aCo_bMn_c]O_d}$ systems, E_{Li}, E_{Ni}, E_{Co}, E_{Mn}, and E_O represent the energy per single atom in the bulk form and a/b/c/d corresponds to the number of single atoms in the structure.

Electrochemical measurement: The detail preparation processes of Ni-rich positive electrode were similar to our previous report.[1] After that, the as-prepared electrodes were further tableted under a pressure of 10 MPa. The positive electrode disks have similar active oxide loading (~5.0 mg cm^{-2} for $\mathrm{LiNi_{0.6}Co_{0.2}Mn_{0.2}O_2}$ and ~4 mg cm^{-2} for $\mathrm{LiNi_{0.8}Co_{0.1}Mn_{0.1}O_2}$. The electrolyte used is 1M $\mathrm{LiPF_6}$ dissolved into ethylene carbonate and ethyl methyl carbonate solvent (3:7 by volume). Lithium metal was utilized as the negative electrode in half-cells. The amount of electrolyte used in the half cells is ~10.0 uL mg^{-1} for cathode material. The amount of electrolyte used in the full cells is ~7 uL mg^{-1} for cathode/anode materials. The electrochemical tests were performed by a LAND instrument (CT−2001A). Electrochemical workstations (CHI660e, Zahner IM6ex) were used for cyclic voltammetry measurement and electrochemical impedance spectra (EIS, 100 kHz and 10 mHz) testing. Galvanostatic intermittent titration technique (GITT) was performed at 1C (1C=180 mAh g^{-1}) for 100s along with the relaxation time of 3600s to reach the quasi-equilibrium potential.

References

1. P. Hou, L. Zhang, X. Gao, *J. Mater. Chem. A* **2014**, 2, 17130–17138.
2. G. Kresse, J. Furthmüller, *Physical Review B* **1996**, 54, 11169.
3. G. Kresse, D. Joubert, *Physical Review B* **1999**, 59, 1758.
4. J. P. Perdew, A. Ruzsinszky, G. I. Csonka, O. A. Vydrov, G. E. Scuseria, L. Constantin, X. Zhou, K. Burke, *Physical Review Letters* **2008**, 100, 136406.
5. S. Dudarev, G. Botton, S. Savrasov, C. Humphreys, A. Sutton, *Physical Review B* **1998**, 57, 1505.
6. J. P. Perdew, K. Burke, M. Ernzerhof, *Physical Review Letters* **1996**, 77, 3865.
7. A. Jain, S. P. Ong, G. Hautier, W. Chen, W. D. Richards, S. Dacek, S. Cholia, D. Gunter, D. Skinner, G. Ceder, *APL materials* **2013**, 1, 011002.

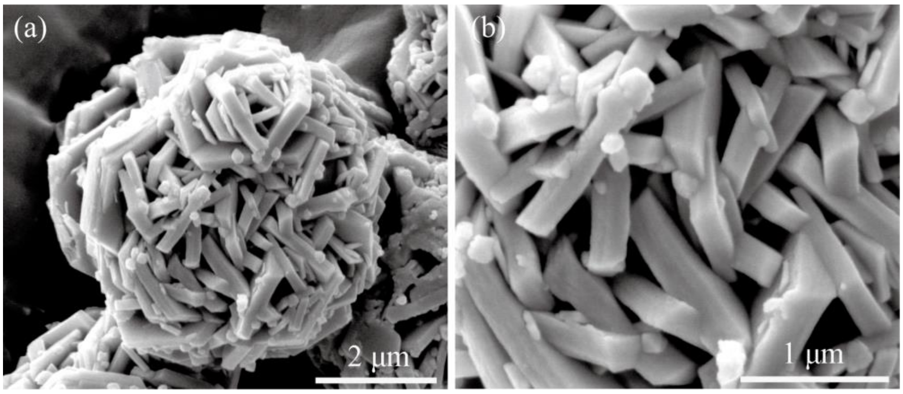

Figure S1 SEM images of the as-prepared Ni-poor $[Ni_{0.2}Co_{0.4}Mn_{0.4}](OH)_2$ precursors by co-precipitation reactions.

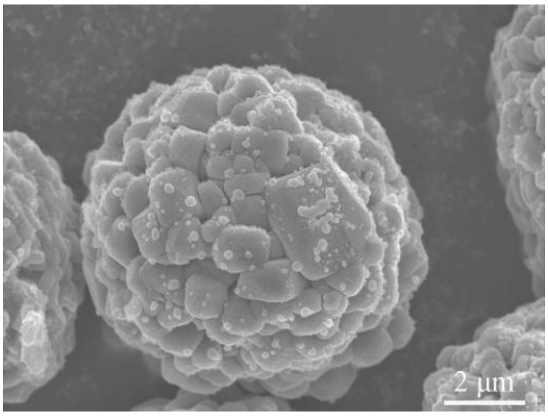

Figure S2 SEM image of as-prepared polycrystalline $Li[Ni_{0.6}Co_{0.2}Mn_{0.2}]O_2$, which was calcined from the mixture of $[Ni_{0.6}Co_{0.2}Mn_{0.2}](OH)_2$ with Li_2CO_3 at 1000 °C for 4h.

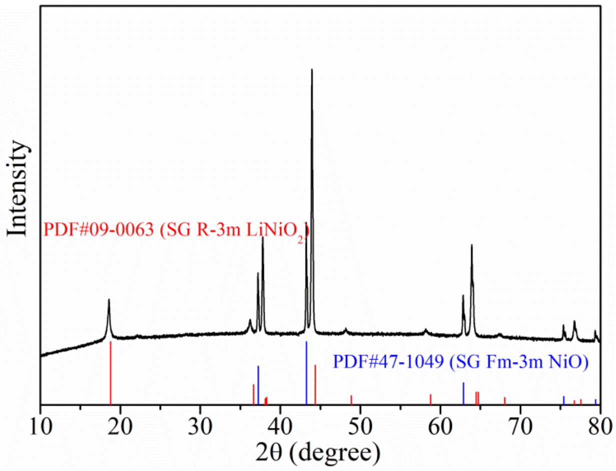

Figure S3 XRD pattern of as-prepared Ni-rich oxide $Li[Ni_{0.8}Co_{0.1}Mn_{0.1}]O_2$ calcined at 1000 °C for 4h.

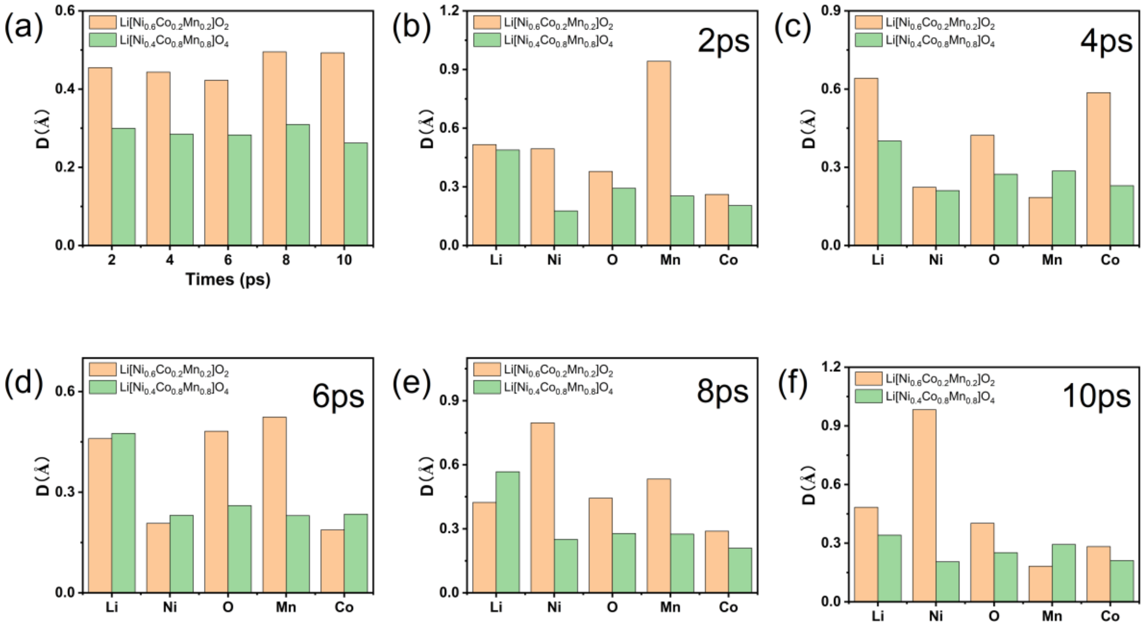

Figure S4 (a) Averaged variation of atomic positions D of all the atoms in Ni-rich layered structure Li[$Ni_{0.6}Co_{0.2}Mn_{0.2}$]O_2 and spinel structure Li[$Ni_{0.4}Co_{0.8}Mn_{0.8}$]O_4 (with respect to atomic positions in the initial structures) from AIMD snapshots at 2, 4, 6, 8, and 10 ps, and (b)-(f) element-specific averaged position variations in each snapshot.

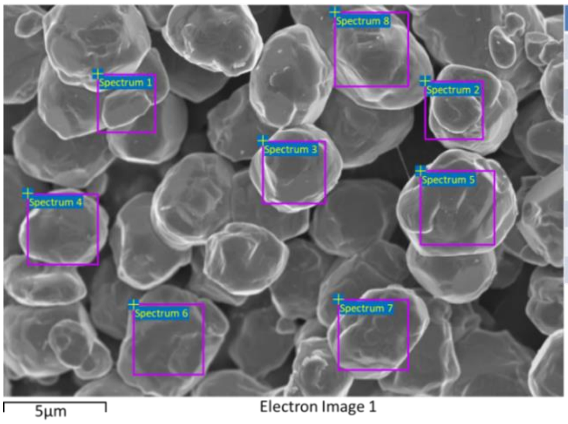

Sites	Atomic ratio of Ni/Co/Mn
1	0.631/0.183/0.186
2	0.622/0.187/0.191
3	0.607/0.195/0198
4	0.603/0.201/0.196
5	0.583/0.206/0.211
6	0.590/0.202/0.208
7	0.593/0.203/0.204
8	0.579/0.209/0.212
Average	0.601/0.198/0.201

Figure S5 EDS results of the single crystal $LiNi_{0.6}Co_{0.2}Mn_{0.2}O_2$ with varied grain sizes from 2 to 5 µm.

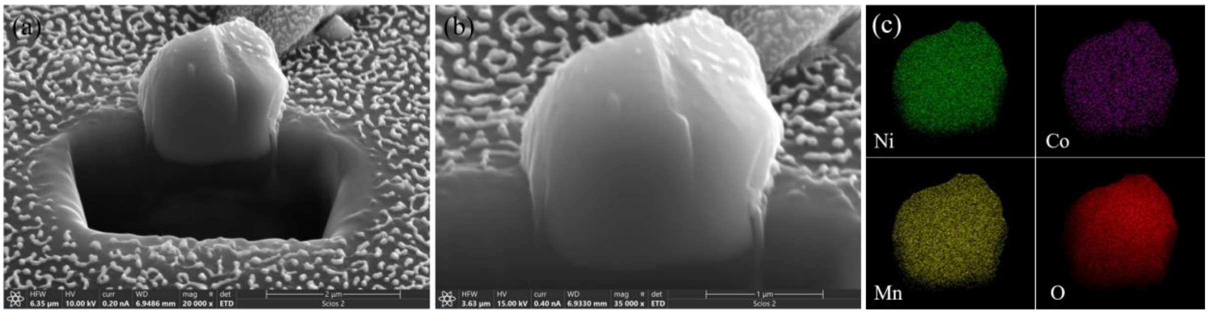

Figure S6 (a,b) SEM images of the cross-section of SC-NCM622 and (C) EDS mapping on this cross-section.

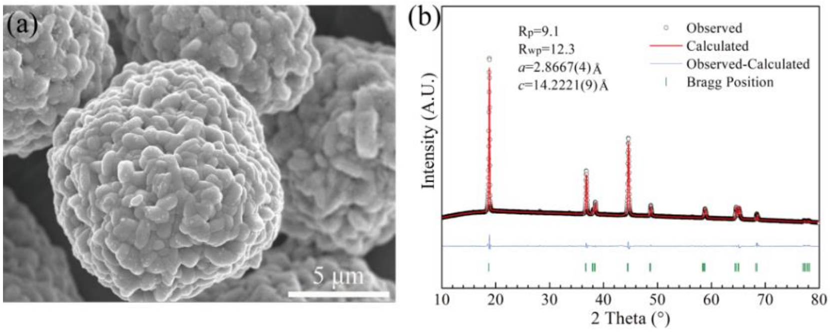

Figure S7 (a) SEM image and (b) XRD of the as-prepared polycrystalline Ni-rich oxide LiNi$_{0.6}$Co$_{0.2}$Mn$_{0.2}$O$_2$. The refined XRD patterns of polycrystalline NCM622 based on LiNiO$_2$ hexagonal (R-3m) phase.

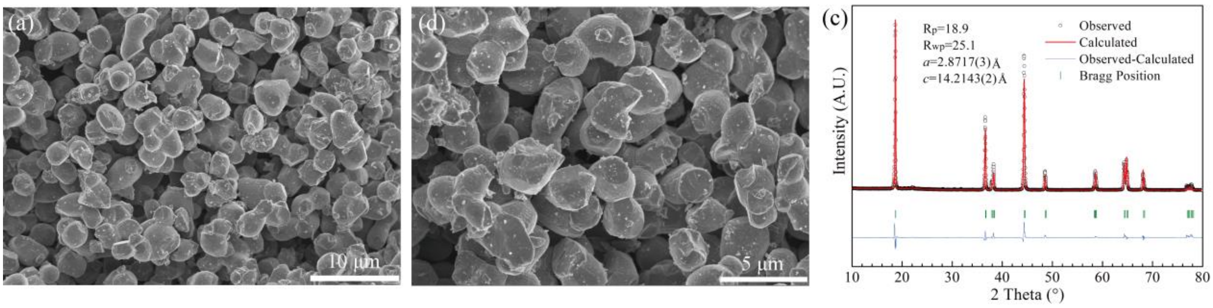

Figure S8 (a,b) SEM images, (c) XRD of the single crystal LiNi$_{0.8}$Co$_{0.1}$Mn$_{0.1}$O$_2$ with the grain sizes from 2 to 5 µm. The refined XRD patterns of SC-NCM811 based on LiNiO$_2$ hexagonal (R-3m) phase.

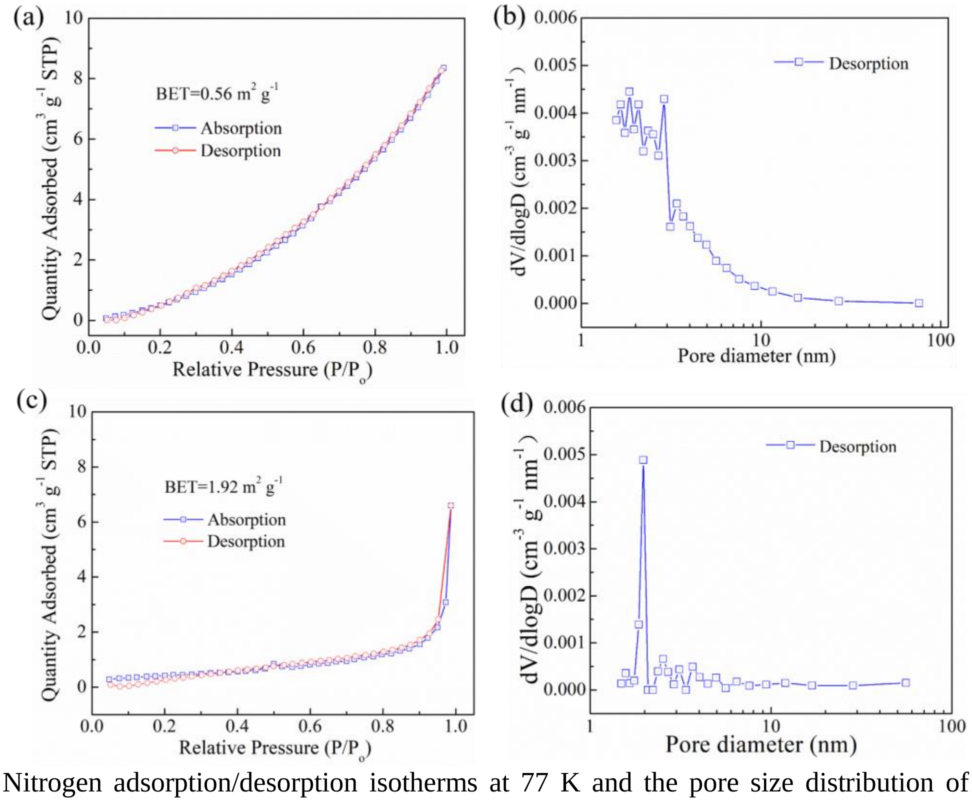

Figure S9 Nitrogen adsorption/desorption isotherms at 77 K and the pore size distribution of (a,b) SC-NCM622 and (c,d) PC-NCM622.

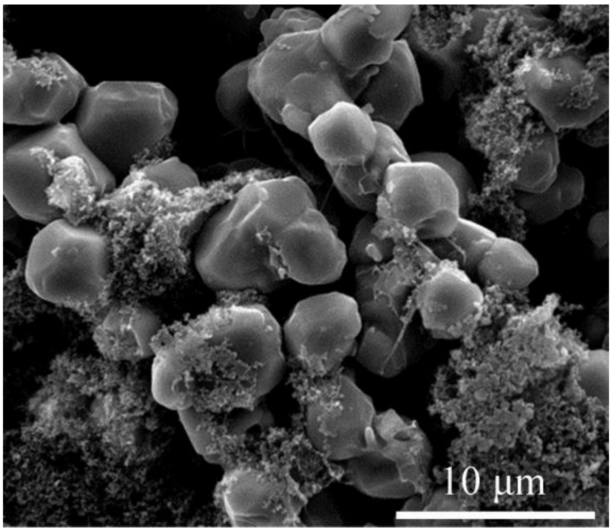

Figure S10 SEM image of the positive electrode consisting of single crystal Li[$Ni_{0.6}Co_{0.2}Mn_{0.2}$]O_2, PVdF and acetylene black. This electrode is tableted under the pressure of 10 MPa.

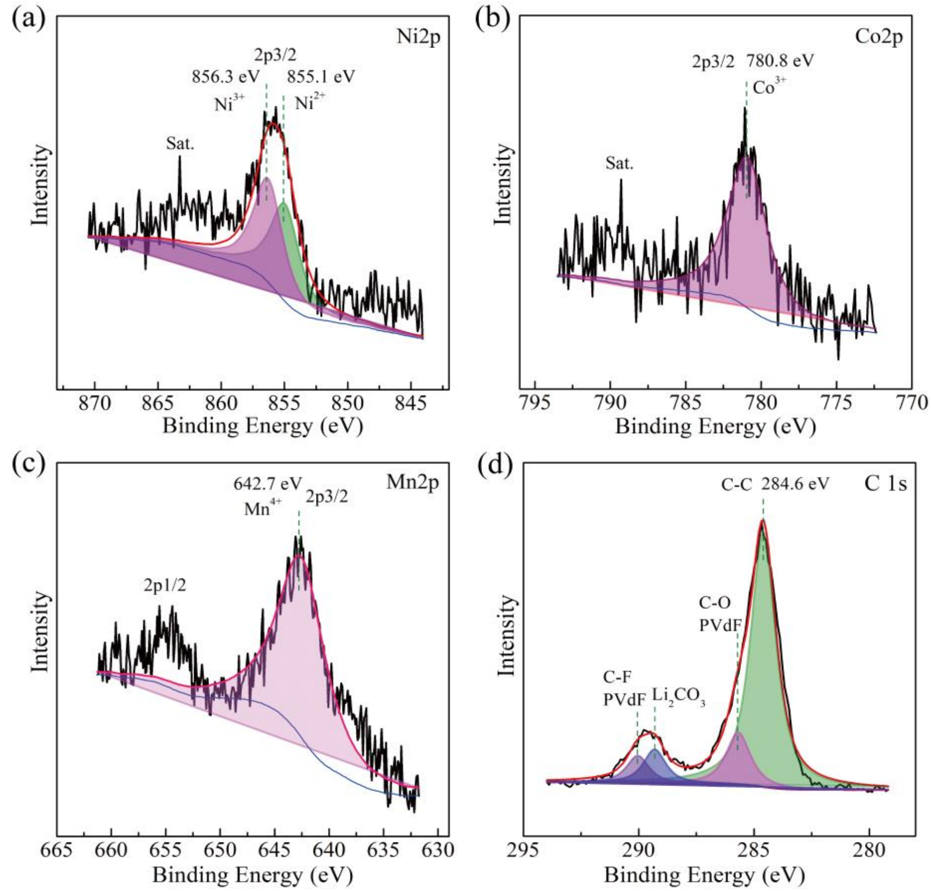

Figure S11 XPS results of single crystal Li[$Ni_{0.6}Co_{0.2}Mn_{0.2}$]O_2: (a) Ni 2p, (b) Co 2p, (c) Mn 2p, and (d) C 1s.

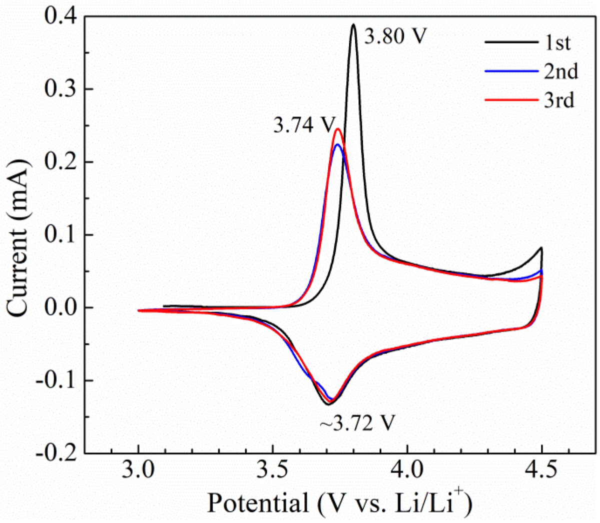

Figure S12 CV curves of single crystal Li[$Ni_{0.6}Co_{0.2}Mn_{0.2}$]O_2 between 3.0 and 4.5 V at a scanning rate of 0.1 mV s^{-1}.

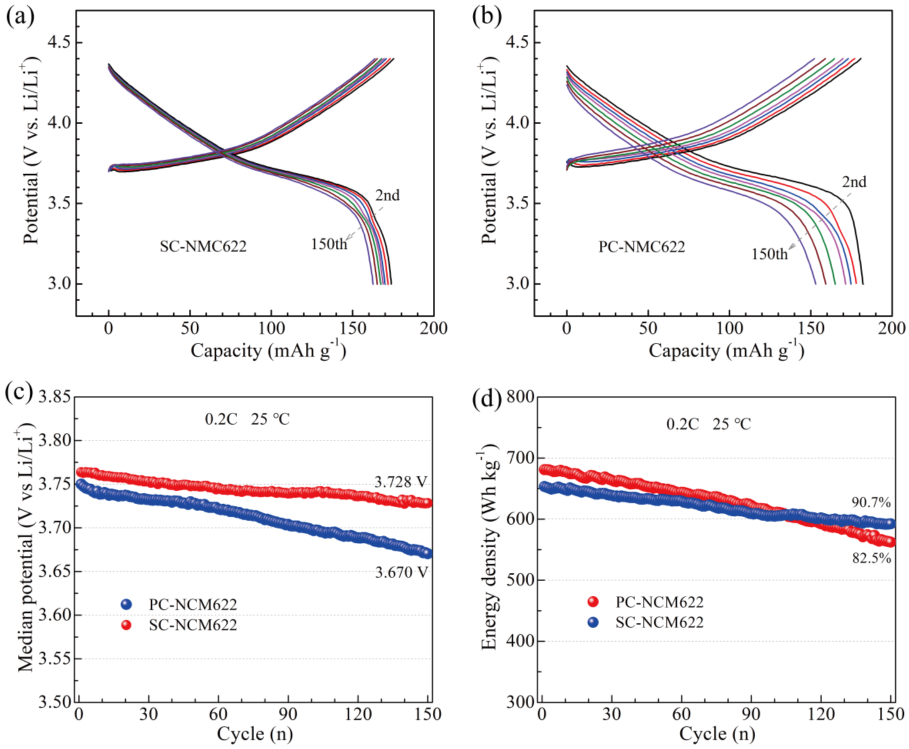

Figure S13 (a) Potential stability of single crystal NCM622 electrode at 0.2C. The continuous charge/discharge curves from 2nd to 100th cycle under the varied upper cut-off voltages: (b) 3.0-4.3 V, (c) 3.0-4.4 V, and (d) 3.0-4.5 V (*vs*. Li/Li^+).

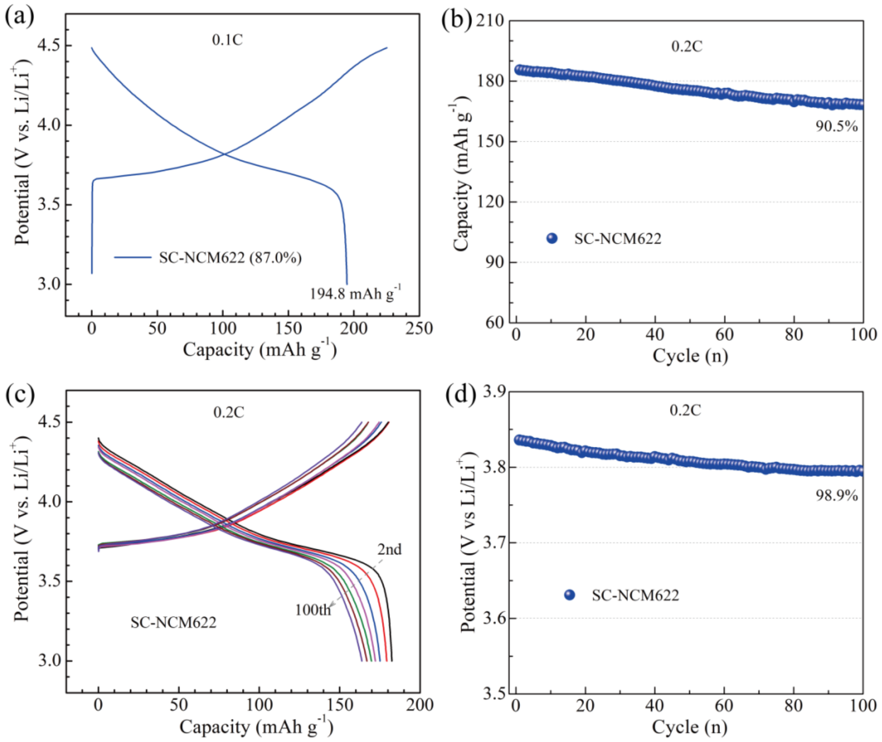

Figure S14 (a) the initial charge/discharge curve, (b) the capacity stability, (c) the continuous charge/discharge curves from 2nd to 100th cycle, and the potential stability of the SC-NCM622 in the voltage range of 3.0-4.5 V (*vs*. Li/Li$^+$).

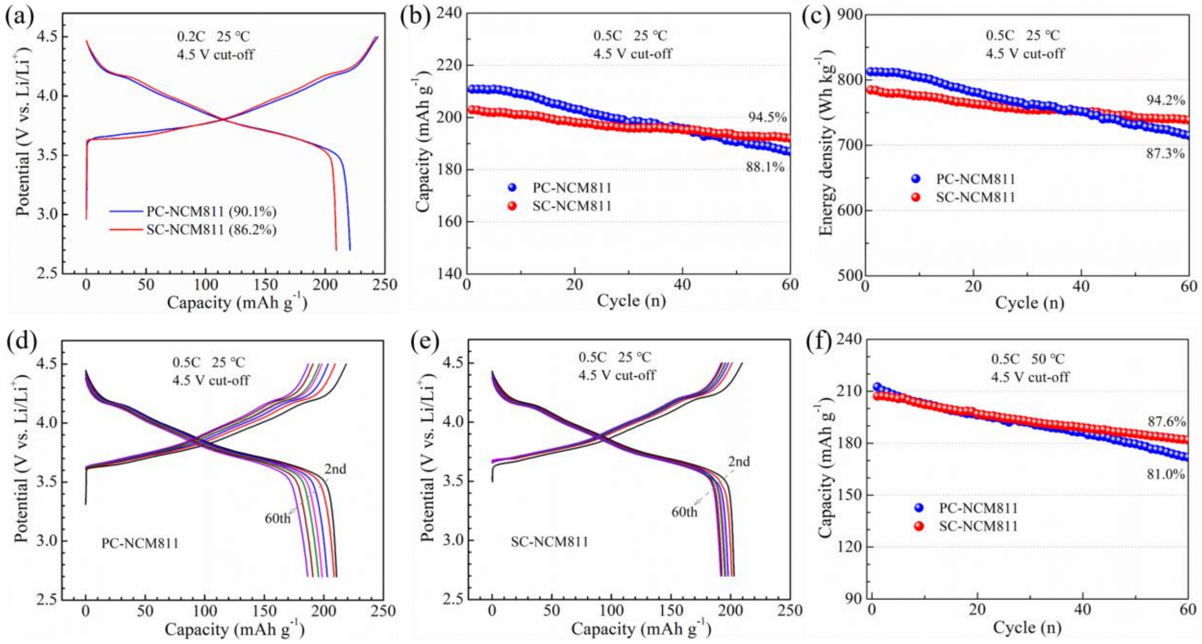

Figure S15 (a) the initial charge/discharge curves, (b) the stability of specific capacity, (c) the stability of energy density, (d,e) the continuous charge/discharge curves from 2nd to 60th cycle at 25 ℃, and (f) the stability of specific capacity at high working temperature of 50 ℃ of both NCM811 in the voltage range of 2.7-4.5 V (*vs*. Li/Li$^+$). The mass loading of active material is about 4 mg cm^{-2}. The roller pressure of both electrodes is ~20 M pa.

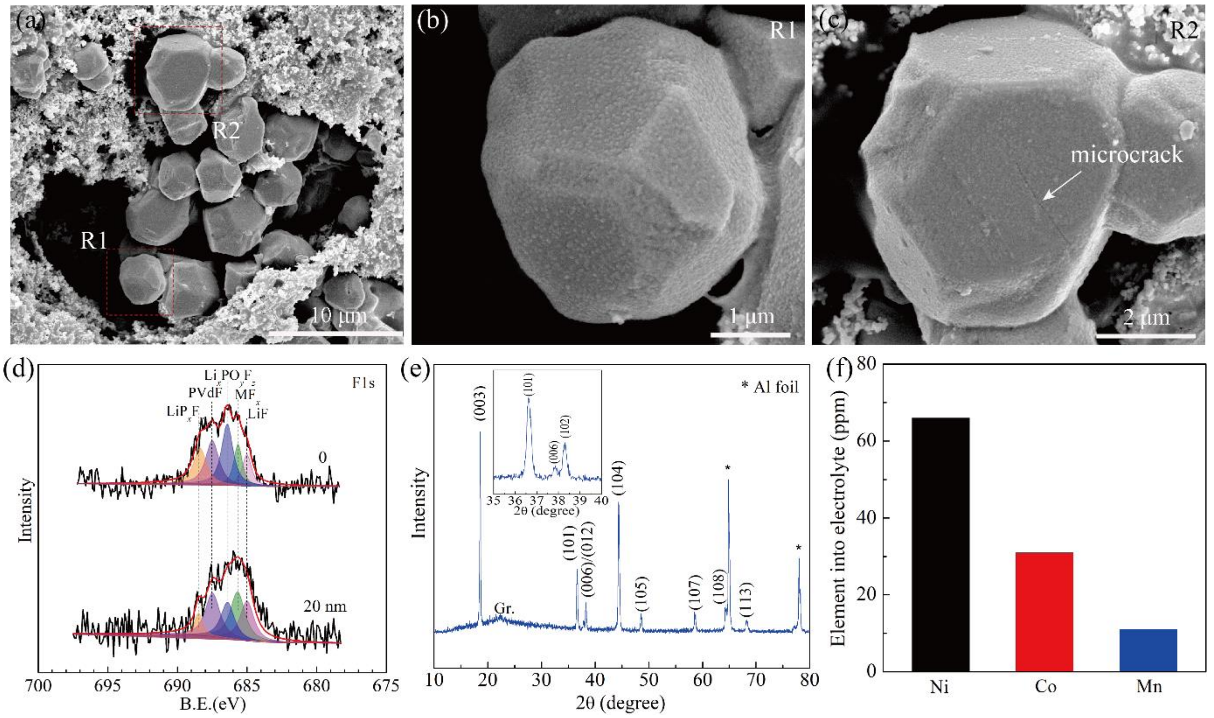

Figure S16 (a-c) SEM images, (d) XPS, (e) XRD pattern, and (f) element dissolution into electrolyte of SC-NCM622 after 100 cycles under the upper cut-off of 4.5 V.

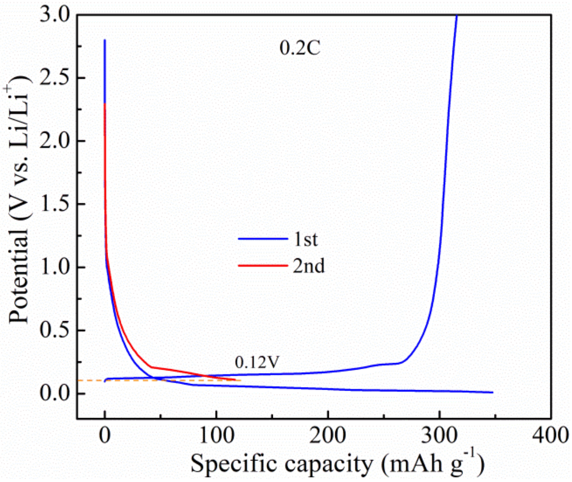

Figure S17 The charge/discharge curves of pre-lithiated mesocarbon microbead (MCMB) anode before using in the full-cells.

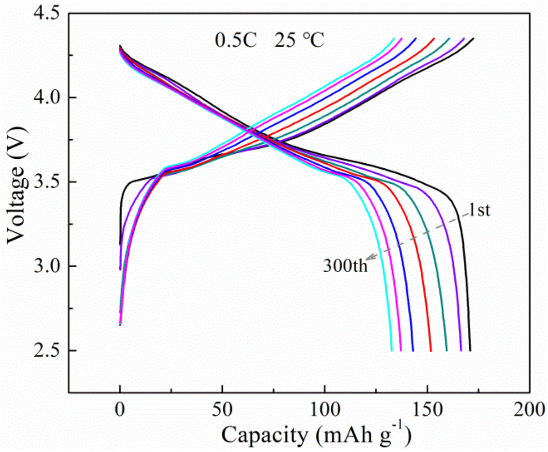

Figure S18 The continuous charge/discharge curves of full cells from 1st to 300th cycle at 0.5 C.

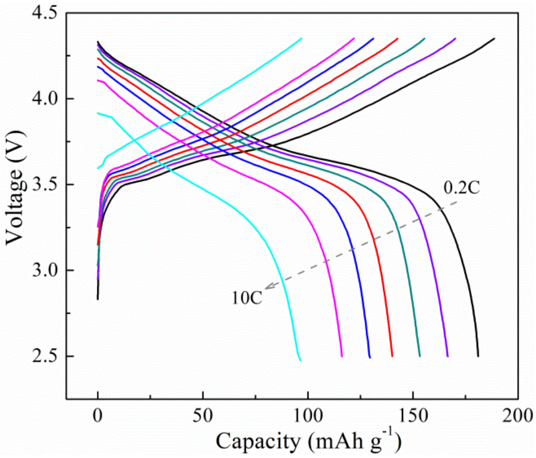

Figure S19 The charge/discharged curves of full cells at different rates from 0.2 to10 C.

Table S1 DFT-calculated surface energy of (001) and (010) facet of layer structure $Li[Ni_{0.6}Co_{0.2}Mn_{0.2}]O_2$ and (010) and (111) facet of spinel structure $Li[Ni_{0.4}Co_{0.8}Mn_{0.8}]O_4$.

Surface energy (eV/Å^2)	(001)	(010)	(111)
$Li[Ni_{0.6}Co_{0.2}Mn_{0.2}]O_2$	0.079	0.086	-
$Li[Ni_{0.4}Co_{0.8}Mn_{0.8}]O_4$	-	0.129	0.101

Table S2 Refined crystallographic parameters by Rietveld analysis for the SC-NCM622.

S. G., R-3m

a=b=2.88658(6), c=14.2227(1)

Atom	Wyck.	x	y	z	Occ.	Them. Fact.
Li1	3b	0	0	0.5	0.968	anisotropic
Ni1	3b	0	0	0.5	0.032	anisotropic
Li2	3a	0	0	0	0.032	anisotropic
Ni2	3a	0	0	0	0.568	anisotropic
Co1	3a	0	0	0	0.200	anisotropic
Mn1	3a	0	0	0	0.200	anisotropic
O2	6c	0	0	0.25859(3)	1.000	anisotropic

R_p=10.2%, R_{wp}=14.7%

Table S3 Refined crystallographic parameters by Rietveld analysis for the PC-NCM622.

S. G., R-3m

a=b=2.8667(4), c=14.2221(9)

Atom	Wyck.	x	y	z	Occ.	Them. Fact.
Li1	3b	0	0	0.5	0.955	anisotropic
Ni1	3b	0	0	0.5	0.045	anisotropic
Li2	3a	0	0	0	0.045	anisotropic
Ni2	3a	0	0	0	0.555	anisotropic
Co1	3a	0	0	0	0.200	anisotropic
Mn1	3a	0	0	0	0.200	anisotropic
O2	6c	0	0	0.25863(1)	1.000	anisotropic

R_p=9.1%, R_{wp}=12.3%

Table S4 The simulated results from EIS of the single crystal NCM622 electrode at varied state of charge and discharge measured after 5 cycles in the potential range of 3.0−4.5 V (*vs.* Li/Li$^+$).

State	Potential (*vs.* Li/Li$^+$)	Simulated electrochemical parameters			
		R_s (Ω)	R_{sf} (Ω)	R_{ct} (Ω)	W_o (Ω)
Charge	3.8 V	1.629	21.47	126.3	306.3
	4.0 V	2.065	20.49	138.2	150.6
	4.2 V	1.73	19.25	152.1	242.5
	4.5 V	0.606	12.44	168.5	1156
Discharge	4.25 V	0.598	14.41	71.67	869
	3.95 V	2.039	24.08	102.7	523
	3.75 V	0.636	17.43	80.7	1465